



Cite this: *Dalton Trans.*, 2018, **47**, 11070

Received 25th June 2018,
Accepted 17th July 2018

DOI: 10.1039/c8dt02586j

rsc.li/dalton

Methyl camouflage in the ten-vertex *closo*-dicarbaborane(10) series. Isolation of *closo*-1,6- $R_2C_2B_8Me_8$ ($R = H$ and Me) and their monosubstituted analogues†

Mario Bakardjiev,^a Oleg L. Tok,^a Aleš Růžicka,^b Zdenka Růžicková,^b Josef Holub,^a Drahomír Hnyk,^c Zbyněk Špalt,^a Jindřich Fanfrlík^c and Bohumil Štíbr^{*a}

Reported are procedures leading to the first types of methyl camouflaged dicarbadeboranes with fewer than eleven vertices. The compounds contain the *closo*-1,6- C_2B_8 scaffolding inside the egg-shaped hepta – decamethyl sheath, which imparts unusually high air and solvolytic stability to all of these compounds.

Introduction

The chemistry of polyalkylated twelve-vertex carboranes, compounds derived from *closo* $[CB_{11}H_{12}]^-$ and $C_2B_{10}H_{12}$, were pioneered by Hawthorne's and Michl's groups.^{1,2} This class of carboranes represents a new genre in organic chemistry, "spherical hydrocarbons" whose icosahedral core is sheathed by a coating of alkyl substituents. In the dicarbaborane area pertinent to this work, the reaction of 1,2- $C_2B_{10}H_{12}$ (*o*-carborane) or 1,7- $C_2B_{10}H_{12}$ (*m*-carborane) with excess MeI in the presence of $AlCl_3$ afforded octamethyl derivatives 1,2,3,6- $H_4C_2B_{10}Me_8$ and 1,2,3,7- $H_4C_2B_{10}Me_8$ in high yield;³ the two positively charged boron positions adjacent to both carbons remain unmethylated. Complete B-methylation was, however, achieved *via* methylation of *p*-carboranes 1,12- $R_2C_2B_{10}H_{10}$ ($R = H, Me$ and Br) with MeOTf/HOTf at reflux for 20 h to cleanly afford the B-permethylated carboranes 1,12- $R_2C_2B_{10}Me_{10}$ in yields over 90%.⁴ These successful experiments, together with those achieved in the methylation of *arachno*-6,9- $C_2B_8H_{14}$,⁵ prompted us to examine a similar methylation strategy in the ten-vertex *closo*-1,6- $C_2B_8H_{10}$ carborane series in which, except for electrophilic halogenation,⁶ no work on B-substitution has so far been reported. In this work we would like to present synthetic

studies on reactions of dicarbaboranes *closo*-1,6- $R_2C_2B_8H_8$ (**1**) (where $R = H$ or Me) with already established methylation agents that lead to permethylation or, at least, to persubstitution on B-vertices.

Results and discussion

Scheme 1 (left) demonstrates that the HOTf-catalyzed MeOTf methylation of the parent *closo*-1,6- $H_2C_2B_8H_8$ (**1a**) dicarbaborane in a Pyrex tube leads at different temperatures (110–175 °C) and varying periods of reaction time (48–120 h) to persubstitution in all B-positions to generate a mixture of the B-permethylated derivative *closo*-1,6- $H_2C_2B_8Me_8$ (**2a**) and the triflate *closo*-1,6- $H_2C_2B_8Me_7$ -8-OTf (**2b**). The mixture was separated by LC on a silica gel support, using hexane and a 10% CH_2Cl_2 -hexane mixture as the mobile phase. The yields of **2a** and **2b** varied in ranges 15–40% and 50–70%, respectively (for approximate yields $\pm 5\%$, see Table 1 and for calculations on the reaction mechanisms, see ref. 7). The table suggests that raising temperatures over shorter reaction time seem to lend support to the formation of the B-permethylated **2a** and **4a**.

An attempt at $AlCl_3$ -catalyzed methylation of **1a** with neat MeI (Pyrex tube, 80 °C, 72 h) yielded, however, only the iodo compound *closo*-1,6- $H_2C_2B_8Me_7$ -8-I (**2c**) (yield $\sim 75\%$) which was isolated and purified, similarly as in the preceding case, *via* LC chromatography. It is evident that the yields of the permethylated **2a** are exacerbated by the formation of the 8-X substituted compounds **2b** and **2c**. As demonstrated on the reaction between **2a** and HOTf in MeOTf (170 °C, ~ 50 h, yield of **2b** 96%), these substituted compounds are likely to be formed as a consequence of electrophilic H^+ -attack by HX evolved in

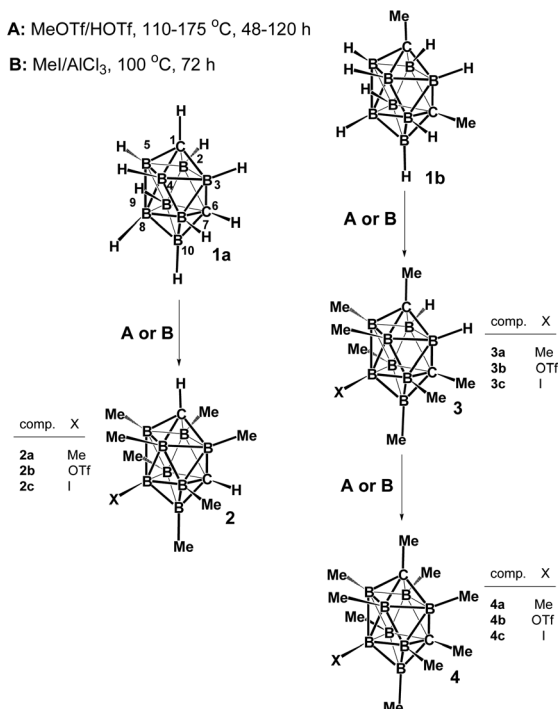
^aInstitute of Inorganic Chemistry, Academy of Sciences of the Czech Republic, Husinec-Řež 1001, Czech Republic

^bDepartment of General and Inorganic Chemistry, Faculty of Chemical Technology, University of Pardubice, Studentská 573, 532 10 Pardubice, Czech Republic

^cInstitute of Organic Chemistry and Biochemistry of the Czech Academy of Sciences, Flemingovo nám. 2, 166 10 Prague 6, Czech Republic

† Electronic supplementary information (ESI) available: NMR data and computed ¹¹B NMR, cartesian geometries. CCDC 1573271 and 1573272. For ESI and crystallographic data in CIF or other electronic format see DOI: 10.1039/c8dt02586j



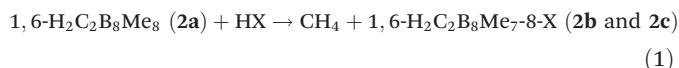


Scheme 1 Synthesis of B-methyl derivatives of the *closo*-1,6- $\text{H}_2\text{C}_2\text{B}_8\text{H}_8$ family.

Table 1 Approximate yields ($\pm 5\%$) of permethylated (2a and 4a) and triflate (2b and 4b) derivatives isolated

Subst.	°C	Time (h)	Yield 2a or 4a (%)	Yield 2b or 4b (%)
1a	110	120	20	70
1a	130	90	25	65
1a	175	48	40	50
1b	110	120	15	70
1b	130	90	15	75
1b	175	48	40	40

the methylation reactions ($\text{X} = \text{OTf}$ and I) at the most negative B8 site⁶ of 2a:



It should be also noted that 2c can be also prepared in 81% yield by MeI/AlCl₃ methylation of the “pre-iodinated” *closo*-1,6- $\text{H}_2\text{C}_2\text{B}_8\text{H}_7\text{-8-I}$ (1c) derivative.⁶

Scheme 1 (right) also shows that the HOTf-catalyzed MeOTf methylation of the C-dimethylated dicarbaborane *closo*-1,6- $\text{Me}_2\text{C}_2\text{B}_8\text{H}_8$ (1b) (110 °C, 120 h) leads only to the octamethylated product *closo*-1,6- $\text{Me}_2\text{C}_2\text{B}_8\text{Me}_6\text{-2,3-H}_2$ (3a, identified by ¹¹B NMR, see Fig. S16†), in which boron positions between both cluster carbon vertexes remain unmethylated, which is probably due to combined sterical and electronic effects of the CMe groups. However, under forcing conditions (15 h, 175 °C), the methylation can be completed to form a mixture of the permethylated *closo*-1,6- $\text{Me}_2\text{C}_2\text{B}_8\text{Me}_8$ (4a) (yield ~15%) with

the triflate *closo*-1,6- $\text{Me}_2\text{C}_2\text{B}_8\text{Me}_7\text{-8-OTf}$ (4b) (yield ~75%) which was separated *via* LC in a 10% dichloromethane/hexane mixture. Nevertheless, the best yield of 4a (~40%) was achieved at 175 °C over a period of 48 h (see Table 1). Unfortunately, an attempt at AlCl₃-catalyzed methylation of 1b with neat MeI (80 °C, 72 h) yielded an inseparable mixture of at least three products, in which the prevailing iodo compound, *closo*-1,6- $\text{Me}_2\text{C}_2\text{B}_8\text{Me}_7\text{-8-I}$ (4c), could be identified by ¹¹B NMR spectroscopy (see Fig. S16†).

The structures of 8-OTf and 8-I-derivatives 2b and 2c were determined by an X-ray diffraction analysis (see Fig. 1 and 2). Their crystallographic parameters thus extend those reported previously for 1b⁸ and 1,6- $\text{H}_2\text{C}_2\text{B}_8\text{H}_7\text{-8-Br}$ ⁶ derivatives of 1. Both compounds adopt Archimedean antiprismatic geometry with apical distances generally shorter than intra- and inter-belt separations, the C–B bond vectors being generally shorter than B–B bonds. The structures unambiguously confirm the B8-substitution along with persubstitution in all other B-positions of the cluster. The crystals of 2a and 4a were not suitable for crystallographic studies and their molecular geometries were therefore optimized at the MP2/TZVP level (Fig. 3 and 4). The optimization revealed that the comparable B–B and B–Me bonding vectors are very similar to those found crystallographically for 2b and 2c. The computation has also led to a good agreement between theoretical and experimental $\delta(^{11}\text{B})$ values for 2a and 4a (max. deviation less than 3 ppm), for the individual values see ESI.†

The HF/cc-pVTZ calculations of the electrostatic potential (ESP) surface show that the parent 1a has hydridic BH vertices which can form dihydrogen bonds,⁹ whereas the hydridic B-bound hydrogens in 2a and 4a are replaced by methyl groups of amphiphilic character.¹⁰ The hydrogen atoms of the

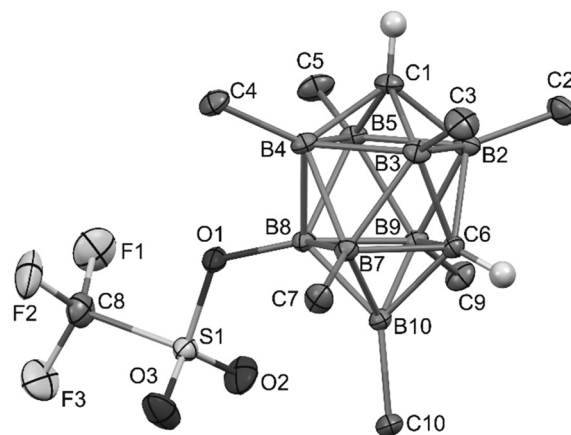


Fig. 1 ORTEP (30% probability level) representation of the molecular structure of *closo*-1,6- $\text{H}_2\text{C}_2\text{B}_8\text{Me}_7\text{-8-OTf}$ (2b). Selected bond lengths (Å): O1–B8 1.473(3), C1–B2 1.594(4), C1–B4 1.606(4), B2–B3 1.888(4), B4–B5 1.867(4), B5–B2 1.839(4), C6–B2 1.744(4), C6–B7 1.772(4), C6–B10 1.621(4), B3–B7 1.808(4), B4–B8 1.829(4), B2–B9 1.810(4), B7–B8 1.826(4), B7–B10 1.728(4), B9–B10 1.728(4), B2–C2 1.569(4), B10–C10 1.571(4); angles (°): O1–B8–B4 112.3(2), O1–B8–B7 103.6(2), B2–C1–B3 72.8(2), B3–C1–B4 110.8(2), B2–B3–B4 89.9(2), B2–C6–B3 65.3(2), C6–B7–B8 84.6(2), B9–C6–B7 97.4(2).

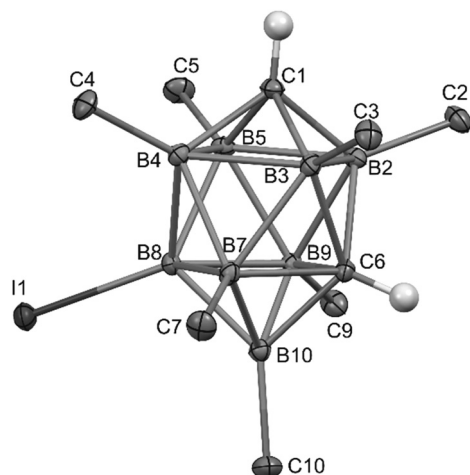


Fig. 2 ORTEP (40% probability level) representation of the molecular structure of *closo*-1,6- $\text{H}_2\text{C}_2\text{B}_8\text{Me}_7\text{-8-I}$ (**2c**). Selected bond lengths (Å): I1–B8 2.176(3), C1–B2 1.596(4), C1–B4 1.615(4), B2–B3 1.896(4), B4–B5 1.879(4), B5–B2 1.851(4), C6–B2 1.746(4), C6–B7 1.774(4), C6–B10 1.620(4), B3–B7 1.807(4), B4–B8 1.828(4), B2–B9 1.806(4), B7–B8 1.821(4), B7–B10 1.724(4), B9–B10 1.720(4), B2–C2 1.569(4), B10–C10 1.564(3); angles (°): I1–B8–B4 119.3(2), I1–B8–B7 129.0(2), B2–C1–B3 72.9(2), B3–C1–B5 111.1(2), B2–B3–B4 89.6(2), B2–C6–B3 65.7(2), C6–B7–B8 85.4(2), B9–C6–B7 96.4(2).

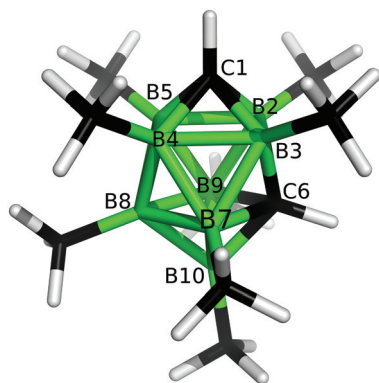


Fig. 3 Molecular model of *closo*-1,6- $\text{H}_2\text{C}_2\text{B}_8\text{Me}_8$ (**2a**) as obtained from the MP2/TZVP optimization. B2–B3 is the longest vector in the molecule, viz 1.889 Å. The other selected internal coordinates are (distances in Å, angles in °): C1–B2 1.593, C1–B4 1.610, B4–B5 1.854, B5–B2 1.843, C6–B2 1.736, C6–B7 1.764, C6–B10 1.623, B3–B7 1.799, B4–B8 1.832, B2–B9 1.800, B7–B8 1.845, B7–B10 1.707, B9–B10 1.707, B2–C1–B3 72.7, B3–C1–B5 110.2, B2–B3–B4 89.5, B2–C6–B3 65.9, C6–B7–B8 85.4.

methyl groups have positive ESP surface and the *exo*-skeletal carbon atoms have negative ESP surface (see Fig. 5). From the viewpoint of electron transmission, the Me groups behave as weak electron acceptors, which might be surprising, as it is opposed to toluene, xylene, hexamethylbenzene *etc.* However, the electron transmission just follows the established electronegativity concept that reflects the fact that *exo*-skeletal substituents are bonded *via* classical 2-centre 2-electron bonds.¹¹ This agrees with the concept elaborated by Viñas *et al.* for a

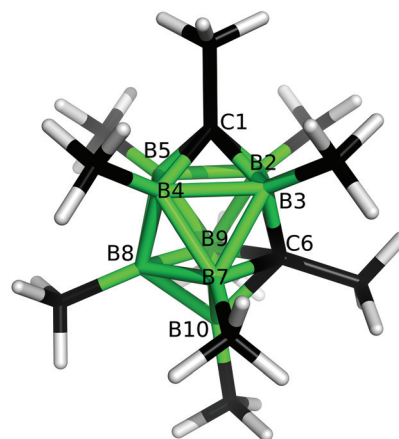


Fig. 4 Molecular model of *closo*-1,6- $\text{Me}_2\text{C}_2\text{B}_8\text{Me}_8$ (**4a**) as obtained from the MP2/TZVP optimization. B2–B3 is the longest vector in the molecule, viz 1.886 Å. The other selected internal coordinates are (distances in Å, angles in °): C1–B2 1.599, C1–B4 1.620, B4–B5 1.851, B5–B2 1.841, C6–B2 1.750, C6–B7 1.799, C6–B10 1.625, B3–B7 1.796, B4–B8 1.837, B2–B9 1.797, B7–B8 1.853, B7–B10 1.705, B9–B10 1.705, B2–C1–B3 72.2, B3–C1–B5 109.1, B2–B3–B4 89.5, B2–C6–B3 65.2, C6–B7–B8 87.1.

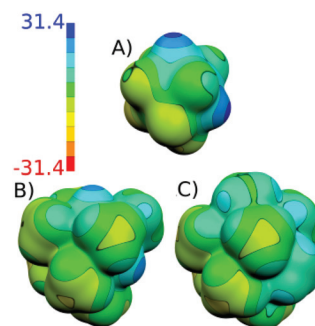


Fig. 5 Computed (HF/cc-pVTZ) electrostatic potential (ESP) surface for (A) **1a**, (B) **2a** and (C) **4a**. The color range of the ESP in kcal mol^{-1}

12-vertex *closo* system.¹² Conceivably, the whole ^{11}B NMR spectra of **2a** and **4a** are significantly paramagnetically deshielded to high frequencies (*i.e.* downfield shifted) with respect to that of **1a**; for the computed ^{11}B NMR spectrum of the latter see ESI.†

The structures of all compounds isolated in this study are also in excellent agreement with the results of multinuclear ^{11}B , [^{11}B – ^{11}B]-COSY,¹³ ^1H , and ^{13}C NMR measurements that led to complete assignments of individual cage BMe, BX and CH units. Graphical inter-comparisons of the ^{11}B NMR spectra of all compounds isolated are in Fig. S15 and S16.† The ^{11}B and ^{11}B – ^1H -decoupled NMR spectra of all B-methylated isomers isolated are identical, exhibiting only singlet resonances, which unambiguously points to persubstitution in all B-vertexes. All the ^{11}B NMR spectra of the C_s -symmetry (a slight gear effect of the Me groups) 2–4 derivatives, exhibiting 1:1:2:2:2 patterns of singlets, are in agreement with the presence of the C1–C6–B10 plane.



The ^{13}C and ^1H NMR spectra of compounds of type **2** and **4** are consistent with the presence of two different CH or CMe and cluster units in positions 1 and 6 (reading upfield) and six or seven, mostly well resolved, Me groups resonating in the high-field area (see comparative Fig. S17 and S18†). Due to the Me-substitution, all the ^{11}B and ^{13}C resonances in the spectra of the B-permethylated compounds **2** are deshielded when compared to those of the B-unsubstituted counterparts of structure **1**, while the corresponding ^1H -resonances of cage CH units are shielded. Similar features can be also traced in the spectra of 8-X compounds with differences attributed to electronic effects induced by OTf and I substituents. The ^{19}F NMR spectra of the triflate compounds **2b** and **4b** are consistent with the presence of one CF_3 group (see Fig. S17 and S18†).

The spectra of the permethylated compounds **2a** and **4a** are exemplified in Fig. 6 and 7 along with signal assignments, for selection of other key NMR measurements see ESI (Fig. S1–S14†).

Of extreme importance for further developments in the field of B-clusters containing less than twelve cage vertices is the question of their resistance to various cage-degradation agents. According to our experience, the ten-vertex dicarbaboranes are most sensitive to the degradation with alcohols. In order to estimate the effect of the Me-sheath, we have tested the behaviour of the **1a/2a** pair to ethanolysis in the presence of a ten-fold excess of EtOH than required by eqn (2) and (3):

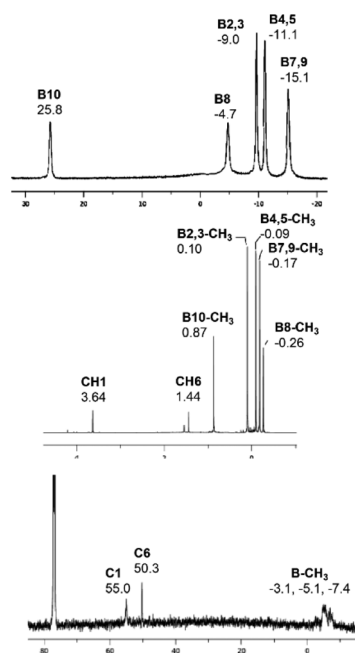
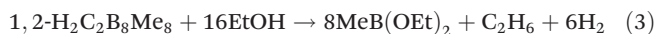


Fig. 6 190.2 MHz ^{11}B , 600 MHz ^1H , and 150.9 MHz ^{13}C NMR spectra of 1,6- $\text{H}_2\text{C}_2\text{B}_8\text{Me}_8$ (**2a**) (CDCl_3).

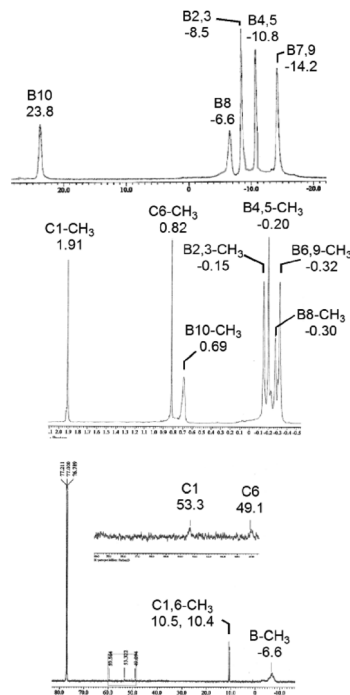


Fig. 7 190.2 MHz ^{11}B , 600 MHz ^1H , and 150.9 MHz ^{13}C NMR spectra of 1,6- $\text{Me}_2\text{C}_2\text{B}_8\text{Me}_8$ (**4a**) (CDCl_3).

The progress of the reactions could be easily monitored by integrated ^{11}B NMR and a two-day treatment with EtOH had no effect to **2a**, while the unprotected **1a** was completely degraded to give $\text{B}(\text{OEt})_3$ over a period of ~ 10 h.

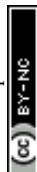
Experimental

Materials and methods

All the reactions were carried out under argon atmosphere. Dichloromethane and hexane were dried over CaH_2 and freshly distilled before use. Other conventional chemicals were of reagent or analytical grade and were used as purchased. NMR spectroscopy was performed at 400 and 600 Mz (for ^1H), inclusive of standard $[^{11}\text{B}\text{-}^{11}\text{B}]\text{-COSY}^{13}$ experiments (all theoretical cross-peaks were observed) leading to complete assignments of all resonances to individual cage B-vertexes. Chemical shifts are given in ppm to high-frequency (low field) of $\Xi = 32.083971$ MHz (nominally $\text{F}_3\text{B}\cdot\text{OEt}_2$ in CDCl_3) for ^{11}B (quoted ± 0.5 ppm), $\Xi = 25.144$ MHz for ^{13}C (quoted ± 0.5 ppm), and $\Xi = 100$ MHz for ^1H (quoted ± 0.05 ppm), Ξ is defined as in ref. 14 and the solvent resonances were used as internal secondary standards. The starting carboranes **1** and **1c** were prepared according to the reported methods.⁶

Dimethylation of *closo*-1,6- $\text{C}_2\text{B}_8\text{H}_{10}$ (**1a**) on carbon vertexes

A solution of **1a** (120 mg, 1 mmol) in dry Et_2O (*ca.* 10–20 ml) was cooled to -78°C and then treated dropwise with 2.5 M LiBu (solution in hexane) (1 ml, 2.5 mmol) under stirring. The



off-white slurry of the Li^+ salt was stirred for additional 1 h prior to dropwise addition of methyl triflate (MeOTf , m.w. 164.1) (410 mg, 2.5 mmol) under cooling down in a dry-ice bath. The mixture was then left stirring for additional 2 h at room temperature. After adding 5% hydrochloric acid (10 ml) under repeated cooling and shaking, the Et_2O layer was separated and evaporated to provide *closo*-1,6- $\text{Me}_2\text{C}_2\text{B}_8\text{H}_8$ (**1b**) (140 mg, 93%) on sublimation. The purity was assessed by ^{11}B NMR spectroscopy (see Fig. S6 and S7†).

***closo*-1,6- $\text{R}_2\text{C}_2\text{B}_8\text{Me}_8$ (2a and 4a) and *closo*-1,6- $\text{R}_2\text{C}_2\text{B}_8\text{Me}_7$ -8-OTf (2b and 4b) (where R = H or Me)**

A solution of carboranes **1a** or **1b** (reaction scale ~ 1.5 mmol) in neat MeOTf (10 ml) was treated with three drops of HOTf and the mixture was heated at different temperatures for varying times in a thick-walled reaction vessel equipped with a Teflon screw cap. In each experiment were the volatiles evaporated and the residue extracted with hexane and filtered through a silica gel plug. The filtrate was then treated with silica gel (~ 5 g) and the hexane evaporated. The residual material was mounted onto the top of a column packed with silica gel ($\sim 2.5 \times 20$ cm) which was then eluted with hexane, followed by a 15% CH_2Cl_2 /hexane mixture to collect two main fractions of R_F (anal., hexane) ~ 0.6 and 0.10 which were identified by ^{11}B NMR and isolated *via* solvent evaporation as compounds **2a**, **2b**, **4a**, and **4b**. Further purification can be achieved by vacuum sublimation at bath temperature $\sim 130^\circ\text{C}$. The isolated yields of individual compounds are in Table 1.

For **2a**: MS (ESI^-): m/z (max.) calcd 233.28, found 233.25; for $\text{C}_{10}\text{H}_{26}\text{B}_8$ (m.w. 232.80) calcd 51.59% C, 11.26% H; found 50.79% C, 11.05% H. For **2b** MS (ESI^-): m/z (max.) calcd 367.21, found 367.30; for $\text{C}_{10}\text{H}_{23}\text{B}_8\text{O}_3\text{SF}_3$ (m.w. 366.84) calcd 32.74% C, 6.32% H; found 32.30% C, 6.11% H. For **4a**: MS (ESI^-): m/z (max.) calcd 261.32, found 261.30; for $\text{C}_{12}\text{H}_{30}\text{B}_8$ (m.w. 260.85) calcd 55.25% C, 11.59% H; found 54.80% C, 11.05% H. For **4b** MS (ESI^-): m/z (max.) calcd 395.24, found 395.25; for $\text{C}_{12}\text{H}_{27}\text{B}_8\text{O}_3\text{SF}_3$ (m.w. 394.89) calcd 36.50% C, 6.89% H; found 36.10% C, 6.58% H.

***closo*-1,6- $\text{H}_2\text{C}_2\text{B}_8\text{Me}_7$ -8-OTf (2b) from *closo*-1,6- $\text{H}_2\text{C}_2\text{B}_8\text{Me}_8$ (2a)**

A solution of compound **2a** (40 mg, 0.17 mmol) in MeOTf (2 ml) was treated with HOTf (204 mg, 1.36 mmol) and heated at 170°C for ~ 50 h in a sealed glass ampoule. The volatiles were then evaporated, the residue dissolved in hexane and filtered through a silica gel plug. The hexane was then evaporated to give 60 mg (96%) of a white crystals which were identified as **2b** as in the preceding experiment.

***closo*-1,6- $\text{H}_2\text{C}_2\text{B}_8\text{Me}_7$ -8-I (2c)**

(a) *From 1a*: A solution of carborane **1a** (122 mg, 1.0 mmol) in neat MeI (10 ml) was heated in a thick-walled reaction vessel equipped with a Teflon screw cap on addition of anhydrous AlCl_3 (ca. 14 mg, 0.14 mmol) at 80°C for 72 hours. The volatiles were evaporated and the residue extracted with hexane. The extract was then treated with silica gel (~ 5 g) and the hexane evaporated. The residual material was mounted atop of

a column packed with silica gel ($\sim 2.5 \times 20$ cm) which was then eluted with 10% CH_2Cl_2 in hexane to collect the main fractions of R_F (anal., hexane) ~ 0.2 which was isolated *via* solvent evaporation and identified by ^{11}B NMR as compound **2c** (269 mg, 78%). Further purification can be achieved by vacuum sublimation at bath temperature $\sim 130^\circ\text{C}$. For **2c**: MS (ESI^-): m/z (max.) calcd 345.16, found 345.12; for $\text{C}_9\text{H}_{23}\text{B}_8\text{I}$ (m.w. 344.67) calcd 31.36% C, 6.73% H; found 30.47% C, 6.51% H. An analogous experiment with **1b** gave a mixture of at least three compounds (350 mg, assessed by ^{11}B NMR) that could not be separated *via* LC. (b) *From 1c*: A solution of the iodo carborane **1c** (51 mg, 0.21 mmol) in neat MeI (3 ml) was heated in a thick-walled reaction vessel equipped with a Teflon screw cap on addition of anhydrous AlCl_3 (ca. 20 mg, 0.2 mmol) at 80°C for 72 hours. Further work-up as in the preceding experiment led to the isolation of 59 mg (81%) of **2c** as a single product which was identified by ^{11}B NMR spectroscopy.

NMR test of resistance toward ethanolysis for *closo*-1,6- $\text{C}_2\text{B}_8\text{H}_{10}$ (1a) and *closo*-1,6- $\text{H}_2\text{C}_2\text{B}_8\text{Me}_8$ (2a)

Compounds **1a** (25 mg, 0.2 mmol) and **2a** (25 mg, 0.1 mmol) were dissolved in ethanol (2 ml) in a NMR tube and both solutions were monitored *via* integrated ^{11}B NMR at ambient temperature. After ~ 10 h exposure the signals of **1a** have completely disappeared (see Fig. S15†) to form $\text{B}(\text{OEt})_3$, while those of **2a** did not change their intensity during 48 h (no formation of $\text{B}(\text{OEt}_3)$ was detected).

Computational details

Magnetic shielding was calculated using the GIAO-MP2 method incorporated into Gaussian09¹⁵ utilizing the IGLO-II basis with the MP2/TZVP geometry and frozen core electrons. Electrostatic potentials were computed at the HF/cc-pVDZ level using Gaussian09 and Molekel4.3¹⁶ programs. It has recently been shown that this basis set size is sufficient for these purposes.¹⁷

X-ray crystallography

The X-ray data for the triflate and iodo derivatives **2b** and **2c** (colourless crystals by slow evaporation of a hexane solution) were collected at 150(2)K with a Bruker D8-Venture diffractometer equipped with Mo ($\text{Mo}/\text{K}\alpha$ radiation; $\lambda = 0.71073 \text{ \AA}$) microfocus X-ray ($\text{I}\mu\text{S}$) source, Photon CMOS detector and Oxford Cryosystems cooling device was used for data collection. The frames were integrated with the Bruker SAINT software package using a narrow-frame algorithm. Data were corrected for absorption effects using the Multi-Scan method (SADABS). Obtained data were treated by XT-version 2014/5 and SHELXL-2014/7 software implemented in APEX3 v2016.5-0 (Bruker AXS) system.¹⁸ Hydrogen atoms were mostly localized on a difference Fourier map, however to ensure uniformity of treatment of crystal, all hydrogen were recalculated into idealized positions (riding model) and assigned temperature factors $\text{H}_{\text{iso}}(\text{H}) = 1.2U_{\text{eq}}$ (pivot atom) or of $1.5U_{\text{eq}}$ (methyl). H atoms in methyl groups were placed with C–H distances of 0.96 while the hydrogen atoms of the C–H in the carborane



cage were assigned according to the maxima on the difference Fourier map. $R_{\text{int}} = \sum |F_o|^2 - F_{o,\text{mean}}|^2 / \sum F_o^2$, $S = [\sum (w(F_o^2 - F_c^2)^2) / (N_{\text{diffs}} - N_{\text{params}})]^{1/2}$ for all data, $R(F) = \sum ||F_o| - |F_c|| / \sum |F_o|$ for observed data, $wR(F^2) = [\sum (w(F_o^2 - F_c^2)^2) / (\sum w(F_o^2)^2)]^{1/2}$ for all data. Crystallographic data for structural analysis have been deposited with the Cambridge Crystallographic Data Centre, CCDC no. 1573271 and 1573272† for **2b** and **2c**, respectively. Crystallographic data for **2b**: $\text{C}_{10}\text{H}_{23}\text{B}_8\text{F}_3\text{O}_3\text{S}$, $M = 366.82$, orthorhombic, $P2_12_12_1$, $a = 10.2153(5)$, $b = 12.7603(7)$, $c = 15.3713(9)$ Å, $\beta = 90^\circ$, $Z = 4$, $V = 2003.65(19)$ Å³, $D_c = 1.216$ g cm⁻³, $\mu = 0.193$ mm⁻¹, $T_{\text{min}}/T_{\text{max}} = 0.3997/0.7455$; $-12 \leq h \leq 13$, $-14 \leq k \leq 16$, $-19 \leq l \leq 19$; 17 134 reflections measured ($\theta_{\text{max}} = 27.12^\circ$), 4409 independent ($R_{\text{int}} = 0.0291$), 4098 with $I > 2\sigma(I)$, 241 parameters, $S = 1.046$, R_1 (obs. data) = 0.0394, wR_2 (all data) = 0.1050; max., min. residual electron density = 0.185, -0.306 e Å⁻³. Flack parameter 0.02(2). Crystallographic data for **2c**: $\text{C}_9\text{H}_{23}\text{B}_8\text{I}$, $M = 344.65$, monoclinic, $P2_1/n$, $a = 7.7088(4)$, $b = 13.5358(7)$, $c = 16.1895(9)$ Å, $\beta = 102.909(2)^\circ$, $Z = 4$, $V = 1646.59(15)$ Å³, $D_c = 1.390$ g cm⁻³, $\mu = 1.919$ mm⁻¹, $T_{\text{min}}/T_{\text{max}} = 0.5122/0.745$; $-9 \leq h \leq 9$, $-17 \leq k \leq 17$, $-20 \leq l \leq 20$; 28 878 reflections measured ($\theta_{\text{max}} = 27.12^\circ$), 3635 independent ($R_{\text{int}} = 0.0263$), 3116 with $I > 2\sigma(I)$, 178 parameters, $S = 1.182$, R_1 (obs. data) = 0.0257, wR_2 (all data) = 0.0811; max., min. residual electron density = 0.472, -1.252 e Å⁻³.

Conclusions

The work is the initial venture into the area of permethylated chemistry of closed cages with fewer than eleven vertices. It was demonstrated that all B-positions in the *closo*-1,6- $\text{R}_2\text{C}_2\text{B}_8\text{H}_8$ (**1**) framework can be furnished with methyl substituents *via* electrophilic reactions with MeOTf and/or MeI reagents. In contrast to its 12-vertex 1,7- $\text{R}_2\text{C}_2\text{B}_{10}\text{H}_{10}$ analogue,³ all the B-positions, inclusive of those between carbon vertexes, can be methylated. The reactions result in permethylated derivatives of **1a** which can be, in fact, viewed as rigid, egg-shaped hydrocarbons with a carborane core inside (see Fig. 5). It should be underlined that such structural arrangements impart an exceptionally high air and solvolytic stability to the otherwise moderately stable compounds **1** by creating a protective methyl sheath around the most sensitive boron section of the molecule.⁵ For example, stability tests have proved that compound **2a** can be quantitatively recovered from ethanolic solution after a 48 h exposure to solvolysis, while the unprotected **1a** is decomposed to $\text{B}(\text{OEt})_3$ over ~10 h ethanolysis, as assessed by ¹¹B NMR measurements. Furthermore, from experience we know that solid **2a** is stable in air for at least two weeks without any noticeable degradation to $\text{B}(\text{OH})_3$. This straightforward enhancement of stability actually brings positive expectations for smaller-cage B-chemistry that was practically abandoned for air-instability as one of the reasons; one might therefore expect new developments in the area of highly alkylated compounds with less than twelve vertexes in the near future. Moreover, Me-substituted derivatives thus far isolated can be used as “Me-labels” for designed syntheses in specific

areas of carborane chemistry, for example in metal-insertion, cluster-rearrangement or cluster-degradation reactions; relevant experiments are being in progress in our laboratories.

Conflicts of interest

There are no conflicts to declare.

Acknowledgements

The work was supported by the Grant Agency of the Czech Republic (project no. 16-01618S).

Notes and references

- For review, see: J. J. Rockwell, A. Herzog, T. Peymann, C. B. Knobler and M. F. Hawthorne, *Curr. Sci.*, 2000, **78**, 405–409.
- (a) B. T. King, Z. Janoušek, B. Grüner, M. Trammell, B. C. Noll and J. Michl, *J. Am. Chem. Soc.*, 1996, **118**, 3313–3314; (b) For review, see: S. Körbe, P. J. Schreiber and J. Michl, *Chem. Rev.*, 2006, **106**, 5208–5249.
- A. Herzog, A. Maderna, G. N. Harakas, C. B. Knobler and M. F. Hawthorne, *Chem. – Eur. J.*, 1999, **5**, 1212–1217.
- W. Jiang, C. B. Knobler, M. D. Mortimer and M. F. Hawthorne, *Angew. Chem., Int. Ed. Engl.*, 1995, **34**, 1332–1334.
- M. Bakardjiev, B. Štíbr, J. Holub, O. L. Tok, P. Švec, Z. Růžicková and A. Růžicka, *Inorg. Chem.*, 2016, **55**, 7068–7074.
- M. Bakardjiev, B. Štíbr, J. Holub, Z. Padělková and A. Růžicka, *Organometallics*, 2015, **34**, 450–454.
- J. Kaleta, A. Akdag, R. Crespo, M.-C. Piqueras and J. Michl, *ChemPlusChem*, 2013, **78**, 1174–1183.
- T. F. Koetzle, F. E. Scarbrough and W. N. Lipscomb, *Inorg. Chem.*, 1970, **9**, 2279–2285.
- J. Fanfrlík, M. Lepšík, D. Hořínek, Z. Havlas and P. Hobza, *ChemPhysChem*, 2006, **7**, 1100–1105.
- (a) C. Esterhuysen, A. Hesselmann and T. Clark, *ChemPhysChem*, 2017, **18**, 772–784; (b) J. Fanfrlík, A. Pecina, J. Řezáč, R. Sedlák, D. Hnyk, M. Lepšík and P. Hobza, *Phys. Chem. Chem. Phys.*, 2017, **19**, 18194–18200.
- In contrast, in the *closo*-1,6- C_2B_8 skeleton the C1 and C6 atoms participate in five multicenter bondings of 3c2e and 4c2e types, which results in their positive charges as opposed to classical electronegativity complex. See: P. Melichar, D. Hnyk and J. Fanfrlík, *Phys. Chem. Chem. Phys.*, 2018, **20**, 4666–4675. Positive charges of *endo*-carbons in *closo* systems were also verified experimentally: D. Hnyk, V. Všetěčka, L. Drož and O. Exner, *Collect. Czech. Chem. Commun.*, 2001, **66**, 1375–1379.
- F. Teixidor, G. Barberà, A. Vaca, R. Kivekäs, R. Sillanpää, J. Oliva and C. Viñas, *J. Am. Chem. Soc.*, 2005, **127**, 10158–10159.



- 13 W. C. Hutton, T. L. Venable and R. N. Grimes, *J. Am. Chem. Soc.*, 1984, **106**, 29–37.
- 14 W. A. McFarlane, *Proc. R. Soc. London, Ser. A*, 1968, **306**, 175–199.
- 15 M. J. Frisch, G. W. Trucks, H. B. Schlegel, G. E. Scuseria, M. A. Robb, J. R. Cheeseman, G. Scalmani, V. Barone, B. Mennucci, G. A. Petersson, H. Nakatsuji, M. Caricato, X. Li, H. P. Hratchian, A. F. Izmaylov, J. Bloino, G. Zheng, J. L. Sonnenberg, M. Hada, M. Ehara, K. Toyota, R. Fukuda, J. Hasegawa, M. Ishida, T. Nakajima, Y. Honda, O. Kitao, H. Nakai, T. Vreven, J. A. Montgomery Jr., J. E. Peralta, F. Ogliaro, M. Bearpark, J. J. Heyd, E. Brothers, K. N. Kudin, V. N. Staroverov, R. Kobayashi, J. Normand, K. Raghavachari, A. Rendell, J. C. Burant, S. S. Iyengar, J. Tomasi, M. Cossi, N. Rega, J. M. Millam, M. Klene, J. E. Knox, J. B. Cross, V. Bakken, C. Adamo, J. Jaramillo, R. Gomperts, R. E. Stratmann, O. Yazyev, A. J. Austin, R. Cammi, C. Pomelli, J. W. Ochterski, R. L. Martin, K. Morokuma, V. G. Zakrzewski, G. A. Voth, P. Salvador, J. J. Dannenberg, S. Dapprich, A. D. Daniels, Ö. Farkas, J. B. Foresman, J. V. Ortiz, J. Cioslowski and D. J. Fox, Gaussian, Inc., Wallingford, CT, 2009.
- 16 (a) MOLEKEL 4.3: P. Flükiger, H. P. Lüthi, S. Portmann and J. Weber, *Swiss Center for Scientific Computing*, Manno (Switzerland), 2000; (b) S. Portmann and H. P. Lüthi, *Molekel: Chimia*, 2007, **28**, 555.
- 17 K. E. Riley, K.-A. Tran, P. Lane, J. S. Murray and P. Politzer, *J. Comput. Sci.*, 2016, **17**, 273.
- 18 G. M. Sheldrick, *Acta Crystallogr., Sect. A: Found. Adv.*, 2015, **71**, 3–8.

